Design of District-level Photovoltaic Installations for Optimal Power Production and Economic Benefit

(Article begins on next page)

Design of District-level Photovoltaic Installations for Optimal Power Production and Economic Benefit

Matteo Orlando, Lorenzo Bottaccioli, Sara Vinco, Enrico Macii, Massimo Poncino and Edoardo Patti
Politecnico di Torino, Turin, Italy. Email: name.surname@polito.it

***Abstract*—PhotoVoltaic (PV) installations are a widespread source of renewable energy, and are quite common urban buildings' roofs. To soften both the initial investment and the recurrent maintenance costs, the current market trends delegate the construction of PV installations to *Energy Aggregators*, i.e., grouping of consumers and producers that act as a single entity to satisfy local energy demand and to sell the surplus energy to the grid. In this perspective, PV installations can be designed with a larger perspective, i.e., *at district level*, to maximize power production not of a single building but rather of a number of blocks of a city. This implies new challenges, including efficient data management (the covered area can be squared kilometers wide) and optimal PV installation (the number of PV modules can be in the order of hundreds or even thousands). This paper proposes a framework to combine detailed geographic and irradiance information to determine an *optimal PV installation over a district, by maximizing both power production and economic convenience*. Our simulation results run on a real-world district prove that the framework allows an advanced evaluation of costs and benefit, that can be used by Energy Aggregators to design a new PV installation, and demonstrate an improvement on power generation up to 20% w.r.t. standard installations.**

***Index Terms*—Photovoltaic installation, PV design, PV optimization, GIS-based design, Zero-Energy District.**

I. Introduction

Among the various Renewable Energy Sources (RES), PhotoVoltaic (PV) energy generation is one of the most interesting solutions, with an estimated market share of 25% of power generation achieved through PV installations by 2050 [1].

The adoption of PV installations is currently encouraged also by the novel market *prosumer* paradigm: energy consumers become also producers, as their residential RES installations not only meet user demand, but generate a potential surplus production that can be sold to the energy grid [2]. While being a promising solution, applying the prosumer paradigm to a single household is not always a viable solution: householders may not afford the cost of installation and maintenance of a PV installation, or may not be willing to make a financial investment in light of possible future earnings.

To overcome this problem, the current market solutions operate at the district level, where a number of buildings cooperate to constitute a larger PV installation and an *Energy Aggregator* (EA) aggregates the overall energy demand and takes care of selling the surplus production to the grid [3]. In this way, single prosumers do not need to care about the investment and the management of the PV systems, still achieving the advantages of potential energy independence [4].

To fully benefit from the new market paradigms, the EA must carefully design the PV installation in the area of interest, so to fully exploit its solar potential. Buildings indeed project shadows that generate heavy partial-shading effects, thus reducing the efficiency of PV power generation and requiring a careful trade-off between the size of installation (with the consequent costs) and the return of investment generated by power generation [5]: it is often the case that a larger PV installation does not lead to larger earnings, as an effect of a larger initial investment and of an ineffective power production in a portion of the installation area, subject to shading effects.

In this scenario, identifying the most suitable roofs of a district to achieve optimal PV power generation and determining the corresponding optimal PV installation is a relevant problem. Not only the problem is complex, but it also requires different skills, ranging from shadow forecast, to PV power generation and optimization, and economic estimation of the return of investment. This work proposes solution to such a complex scenario with *a framework that works at district level to determine the optimal PV installation* from the perspective of both costs/benefit trade-off and of production efficiency.

The novelty of this work lies in the following contributions:

- a GIS-based approach is used to evaluate the evolution of irradiance and temperature over the roofs of a district over one year, by achieving a good spatial resolution ($1m$) to allow an accurate estimation of the operating conditions of a possible PV installation, still operating on a wide urban area (in the order of squared kilometers);
- the identification of the optimal placements of PV modules over the district, achieved by considering the roofs of district as a whole, i.e., allowing to connect PV modules located on contiguous roofs of different buildings;
- an economic analysis to determine the payback time of the PV installation;
- a trade-off analysis that considers the payback time and the return of investment of the installation, different sizes of the PV installation and allowing different levels of PV efficiency, to determine the most suitable and the most economically convenient solution in the interest of the EA;
- the application to a district located in Turin, Italy, that will prove an improvement of power production of up to 20% and of 25% of payback time w.r.t. a traditional installation.

The paper is organized as follows. Section II reviews relevant literature solutions, and section III provides the necessary background on PV power generation. Section IV presents the proposed methodology. Section V discusses the experimental results. Finally, Section VI provides our concluding remarks.

II. State of the Art

The placement and installation of PV power sources has been widely studied in the literature, with the goal of both optimizing power production and sizing, and its relation with the grid [6]–[8]. In this scenario, the adoption of Geographic Information System (GIS) technologies is essential to enable the simulation of PV production in real urban environments, starting from either a Digital Surface Model (DSM) or a 3D city model of the area of interest [9]–[11]. The works in [12]–[14] analyze the potential energy production of wide areas, such entire islands or regions: they use GIS tools to extract irradiance information about the area of interest, to estimate the most promising portion for PV installation. Their analysis however does not take into account roofs, but it rather focuses on geographic areas. The works proposed in [9], [15] focus on a smaller scale, i.e., district-level, to estimate the solar potential of different roofs and calculate the expected energy production. However, both these works estimate the energy production considering a standard PV installation, without taking advantage of fine grained information to maximize such production. Other works, like [16], [17], further restrict the perspective to a single roof: they uses detailed historical data of irradiance to evaluate the best rooftop PV installation by focusing on single household installations, thus not taking the full advantage of the district-level perspective.

With respect to the literature, this work proposes a framework to investigate a relatively wide area of a urban context ($\sim 1.7km^2$ in our experimental analysis) to find a possible optimal configuration of a PV installation. The framework exploits a high resolution Digital Surface Models (DSM) and historical weather data to identify the most promising positions for PV installation, considering the possibility to connect PV modules located on contiguous roofs. Each explored solution is used to make an estimation of its Payback Time (PT) to provide a tangible economic indicator for the EA, that thus can take full benefit from the installation in terms of return of investment and of generated power.

III. Photovoltaic Power Generation

A PV module is an assembly of photo-voltaic cells using solar irradiance as a source of energy to generate direct current electricity. A PV module is described by a voltage-current (I-V) characteristic curve (left of Figure 1, black lines), which changes as a function of the irradiance G: current and voltage production increase proportionally to G. The maximum of the corresponding voltage-power (P-V) curves (grey lines) corresponds to the optimal conditions for extracting power, given the current irradiance.

In any PV installation PV modules are typically connected in series or in parallel to achieve the desired voltage and

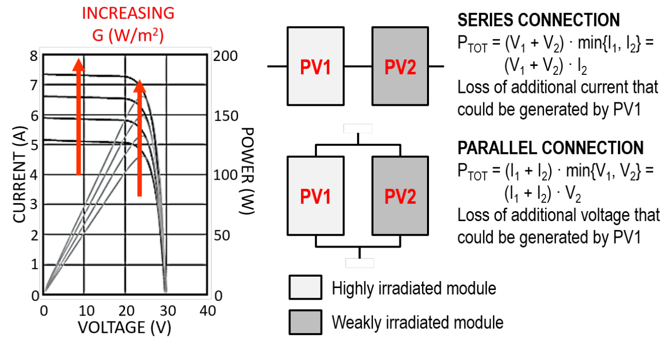

Fig. 1. Typical voltage-current (I-V, black) and voltage-power (P-V, gray) curves of a PV module [18] (left), and impact of partial shading on the series or parallel connection of PV modules (right).

current levels (right of Figure 1). The typical connection is organized as a number of parallel strings, each composed of the same number of PV modules connected in series.

If two connected PV modules work with the same input irradiance, then their connection doubles the output power production. However, this is rarely the case, above all in urban areas where obstacles such as chimneys, surrounding buildings, trees, etc project shadows and determine a heterogeneous distribution of irradiance [19]. Shading is critical for PV installations, as the least irradiated PV module acts as a bottleneck on power production: the higher the variance of irradiance, the higher the power loss (right of Figure 1). When PV modules are connected in series, the least irradiated module will provide the smallest current; when PV modules are connected in parallel, the PV module with lowest voltage will determine the voltage of all connected PV modules.

IV. Methodology

The goal of the paper is to find the best possible configuration for a PV installation for a district of a city, considering the possibility to connect PV module across contiguous roofs. The solution adopted to achieve this result is based on five main steps. The first step identifies the area of the district suitable for the installation of PV modules. Then, we proceed with the generation of the traces of G and T for the whole area with a fine time and space resolution (A). In the second step, we evaluate a statistical measure to find which points of the suitable area are the most illuminated during the year, and thus the most promising from the perspective of power production (B). The third step consists in the placement of PV modules to find the optimal configuration (C). Given such a placement, we evaluate the yearly production (D) and the payback time (E) to allow comparison between different solutions.

A. Suitable area and irradiance

Starting from a Digital Surface Model (DSM) of the district, the algorithm identifies possible encumbrances and the corresponding evolution of shadows to find areas which could be used for the deployment of the PV installation.

To process the DSM, we used GDAL [20], a translator library for raster and vector geospatial data formats. This allowed to identify the surfaces (i.e., roofs) that maximize power production in terms of tilt angle and orientation, depending on the geographic location of the district. In our case study, we generated two raster images in GeoTIFF format: one to store the data describing the roof slope and the other to store the data of the aspect for the area under test. Then we processed these two files to extract the surfaces with a slope between 15 and 36 degrees and aspect value between 240 and 300 degrees in order to have roof pitches oriented towards South, configuration that guarantees optimal sun exposition and potential PV production [21]. Top of Figure 2 shows an example roof (pink) to highlight how the area that is suitable for PV installation resulting from this step (purple) is only a portion with respect the whole area.

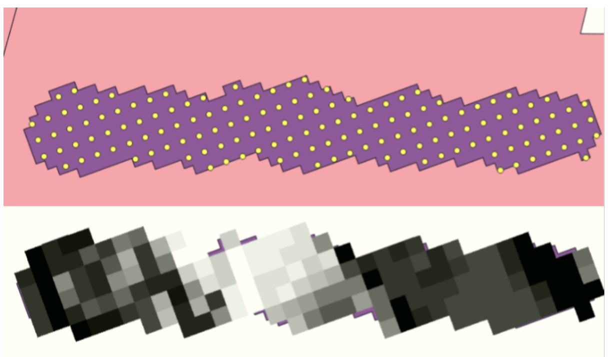

Fig. 2. Example of total area of a roof (pink), area suitable for PV module placement (purple), and DSM points covered by the area (yellow) (top), and corresponding 75th percentile over one year of the suitable area (bottom, darker areas are subject to more shading and thus to lower irradiance).

Each identified suitable area is then annotated with the inclination and the aspect of its roof pitch. Those areas are then intersected with cadastral maps to annotate the average height of the roofs. This information is extremely useful as the height difference of contiguous roofs must be taken into account when the placement algorithm is executed, to allow installation of connected PV modules on different roofs without incurring in high dispersion of the produced power.

The areas are then sampled with the same resolution of the DSM (i.e. $1m$). The result of this sampling is shown in top of Figure 2, where each point (yellow) corresponds to a pixel of the DSM model that resides within the area. Using these points, we are able to determine the evolution of irradiance over time from yearly weather data by using the shadow model developed in [22]. Using georeferenced points allows to generate and store data only for the areas that could actually be exploited for the installation of the PV modules. This is a key point of the proposed approach, as it allows to optimize the amount of data that must be generated, memorized and handled thus guaranteeing an optimal trade-off between the size of the district of interest (that can be of a number of squared kilometers) and achieving at the same time a fine-grain representation of the solar evolution of the suitable areas over time.

B. Performance pre-evaluation

The next step consists of identifying the most irradiated portions of the suitable areas, that are the most promising positions for the installation of PV modules. The suitable area is explored by considering all possible placements of a PV module inside of the area. The yearly trace of irradiance of a position is derived from the DSM by considering the traces for the DSM point covered by the PV module. In case there are multiple points, for each time instant we consider the minimum value of the irradiance over all the traces, to reproduce the bottleneck effect described in Section III.

To get a compact signature and allow easy comparison of positions, we use the *75th percentile of irradiance*, i.e., the value below which 75% of samples of a yearly irradiance traces fall. The 75th percentile thus allows to discriminate between highly irradiated and poorly irradiated positions, as larger values of the percentile identify positions whose irradiance trace distribution is more skewed towards the upper range of the irradiance values, i.e., that are more irradiated and more promising for PV power production. Figure 2 exemplifies this process by showing a suitable area and its heat-map, where whiter points corresponds to a higher value of the 75th percentile (i.e., more irradiated points).

The PV module positions are then sorted by decreasing value of the 75th percentile. The user is now allowed to give a threshold value $minTh$ representing the minimum value of the percentile that is accepted for PV placement. The experimental analysis will prove the impact of this choice on the resulting identified solution. All positions with 75th percentile lower than $minTh$ are now excluded from the suitable area, as the performance indicator identifies them as non-promising locations from the perspective of PV power generation. The resulting suitable area represents the area that can be occupied by PV modules to achieve optimal power generation.

C. Optimal Placement algorithm

The third step consists of the identification of an optimal placement for the identified suitable area, given the list of PV module positions sorted by decreasing value of 75th percentile.

The algorithm starts from the position with highest 75th percentile, and goes through the sorted list to identify other positions that can be used, given the following constraints:

- no overlap with already placed PV modules;
- distance from the already placed PV modules below a threshold $maxD$;
- height difference w.r.t. already placed PV modules below a threshold $maxH$.

The constants $maxD$ and $maxH$ are determined by the user and they allow to connect PV modules placed on contiguous roofs or roof pitches, but ensure that the necessary cables do not generate high dispersion. This step is repeated until one series of S PV modules is built. Any time that a new position is chosen, it is removed from the sorted list.

Once that a series of size S is built, the positions excluded due to distance and height constraints are put back in the sorted list, and the algorithm starts the construction of a new series from the new position with highest 75th percentile. The algorithm ends when it is not possible to build a new series, i.e., the number of remaining positions is lower than S.

The resulting organization of the PV installation is made of a number of series made of S PV modules each, connected in parallel. It is important to note that the greedy approach adopted by the algorithm allows to connect in series PV modules with similar irradiance distribution, thus reducing the bottleneck effect caused by partial shading.

D. Power production

The last step is the evaluation the yearly power production for the identified optimal PV installation. To achieve a measure of performance, the algorithm generates also a traditional placement of the same number of PV modules, by positioning them in the suitable area but with a more standard positioning (i.e., a "compact" rectangular placement that does not consider the 75th percentile of irradiance).

The yearly trace of each PV module is used to estimate the yearly power production of the overall PV installation by considering the series and parallel connections between PV modules. Given N the number of series identified in step IV-C and S the number of PV modules composing each string, the resulting power of the whole installation P_{yearly} is thus derived with the following formula, reproducing the bottleneck effect mentioned in Section III:

$$\begin{cases} P_{panel} & = & V_{yearly} \cdot I_{yearly} \\ V_{panel} & = & \min_{j=1,\dots,N}(\sum_{i=1,\dots,S} V_{module,ij}) \\ I_{panel} & = & \sum_{j=1,\dots,N}(\min_{i=1,\dots,S} I_{module,ij}) \end{cases}$$

where $V_{module,ij}$ and $I_{module,ij}$ are the voltage and current extracted from the i-th PV module in the j-th string, and T is the length of the irradiance traces.

E. Economic analysis

The economic effectiveness of a PV installation is usually determined as its financial Payback-Time (PT), i.e., how much time it takes for the total savings and revenue streams to cover the total cost of the initial installation. It thus indicates the number of years of operation needed to payback the initial investment when considering also maintenance costs by using the following formula:

$$PT = \frac{I_c}{R_y - M_y}$$

Where I_c is the installation cost, R_y are the yearly revenue generate by selling all the energy produced to the grid (calculated by multiplying the yearly kWh production P_{yearly} of a configuration per E_p that is the price at which the energy is sold to the grid), M_y is the yearly maintenance cost due to the price of cleaning, monitoring, and repairing that needs to be applied periodically an efficient system.

Fig. 3. Satellite view of the area used for the test

V. Results

A. Suitable area identification and optimization

We tested the proposed framework on a district of the city of Turin represented in Figure 3. The satellite view of the area used for the test is overlapped with the result of step IV-A: the green area represents the total surface of the roofs (around $1.7km^2$), while the red area represents the area that is suitable for PV installation (about $8,340m^2$). It is interesting to notice that just 0.5% of the available roof surface is considered suitable for PV installation. This underlines that the DSM data management strategy followed in this work allows to optimize data memorization, as only few DSM points are used to filter the suitable area, and full irradiance traces are generated only for a very limited portion of the district.

B. Optimal placement setup

In our setup, we consider a PV-MF165EB3 module by Mitsubishi [18] organized in strings of $S = 8$ PV modules. The algorithm is set to allow maximum distance among PV modules on the same series $maxD = 3m$ and a maximum height difference $maxH = 0.5m$. This configuration allows to place in the same series PV modules positioned on different but almost contiguous roofs. An example of this scenario is visible in the top of Figure 4, that zooms on a portion of the district to show an example where the suitable area spans across two contiguous roofs (delimited by the black line in Figure 4).

C. Analysis of the identified PV placements

To test the performance of the placement, we executed the algorithm multiple times with different values of $minTh$, i.e., the threshold of the 75th percentile used to consider only the most promising portion of the suitable area. The results are reported in Table I. When increasing $minTh$, the area considered promising is reduced as a number of suitable locations are removed as featuring a 75th percentile lower than $minTh$. Thus, both the percentage of exploited area and the number of placed PV modules decrease when increasing

TABLE I
PERCENTAGE OF AREA USED BY PV PLACEMENT OVER THE TOTAL SUITABLE AREA WHEN VARYING $minTh$

Threshold $minTh$ (W/m^2)	PV modules (#)	Installation area (m^2)	Suitable area used (%)
100	1,792	1,540	21
200	1,536	1,319	18
300	656	561	8
400	464	394	6
500	176	148	2

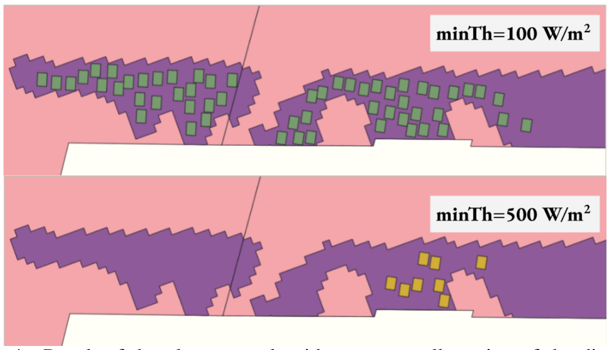

Fig. 4. Result of the placement algorithm on a small portion of the district (i.e., two roofs) with threshold $minTh = 100\ W/m^2$ (top) and $minTh = 500\ W/m^2$ (bottom): the pink area represents the area of the roofs, the purple area is the suitable area, and the rectangles represent PV modules placed on locations with 75th percentile higher than $minTh$. As expected, the second placement contains less PV modules, as the minimum threshold is set to a higher value.

$minTh$. An example is shown in Figure 4: when $minTh$ is set to 100 W/m^2 , 21% of the available surface is considered suitable for PV placement; when $minTh$ is increased to 500 W/m^2, only 2% of the area is considered suitable for PV installation, and as a result far less PV modules (colored rectangles) are installed on the same portion of roof. If we plot the number of PV modules installed (first plot in Figure 5), we can observe that the decrease is not linear w.r.t. the threshold: as an example, moving from 200 to 300 W/m^2 the number of modules (and the area exploited) are reduced by $2/3$, as a wide percentage of locations has 75th percentile between 200 and 299 W/m^2. As expected, the initial installation cost decreases according to the number of PV modules installed (second plot in Figure 5).

D. Energy production performance

To analyze the performance of the proposed algorithm in terms of power outcome, we compared the yearly production of the identified optimal placements w.r.t. a traditional placement of the same number of PV modules. The traditional placement is built by installing PV modules in a more standard positioning (i.e., a "compact" rectangular placement that does not consider the 75th percentile of irradiance) by individually considering each roof, thus avoiding cross building deployments.

Table II shows that the production of the optimal PV installations is always larger than the one of the corresponding traditional placement, and as expected the production of the different configuration decreases linearly with the number of modules installed. However, it is interesting to notice that the improvement of power production is higher with higher values of $minTh$, with maximum improvement of 21% with threshold 500 (as shown in Table II and reported in the third plot of Figure 5). This behaviour can be easily explained by considering that the lower the threshold the higher the number of PV modules, and thus of potential overlap of positions of PV modules for the two placements. Vice versa, with higher thresholds the number of PV modules is reduced and the optimal placement can successfully select only the positions less affected by shading. This reduces the impact of the bottleneck effect of partial shading on the output power production of the optimal PV placement. This analysis is confirmed by the amount of area shared by the two placements, that is higher with $minTh = 100\ W/m^2$ (36%) and decreases with higher values of $minTh$, with a minimum of 15% with $minTh = 500\ W/m^2$.

TABLE II
SUMMARY OF THE COMPARISON AMONG THE OPTIMAL PLACEMENT WITH VARYING $minTh$ W.R.T. A TRADITIONAL PLACEMENT OF THE SAME NUMBER OF PV MODULES.

Threshold $minTh$ (W/m^2)	PV modules (#)	Shared area (%)	Power production (MW)		
			Optimal	Traditional	(%)
100	1,792	36	1,015	998	+1.6%
200	1,536	31	905	874	+3.6%
300	656	22	423	376	+12.6%
400	464	23	323	277	+16.9%
500	176	15	139	115	+20.8%

E. Payback time

Using the procedure explained in IV-E we evaluated the PT for both the classic and the optimal configuration considering also the different value of the threshold. The energy price considered is 0.22€ per kWh [23], the cost is 250€ per PV module and the maintenance cost considered is 15€ per PV module per year. The plot 4 in Figure 5 shows how the PT decreases together with the number of PV modules and that the payback times of the PV installation produced by our framework are always lower than the classical ones. In particular when the threshold is at 500 W/m^2 the configuration produced by the framework reduces by $1/4$ the PT. However by comparing the result in Table II and the Figure 5 we can notice while increasing the amount of PV modules increases the production and therefore the earning this does not decrease the PT that instead increases. This underlines how this kind of analysis are useful for an EA that needs to take into account this economic analysis to plan his investment.

VI. CONCLUSIONS

The paper proposed a framework to support optimal installation of PV modules in a city district, with the goal of maximizing the profit for an EA. The approach is based on an efficient management of DSM data, that generates detailed irradiance traces only for the promising portion of the district

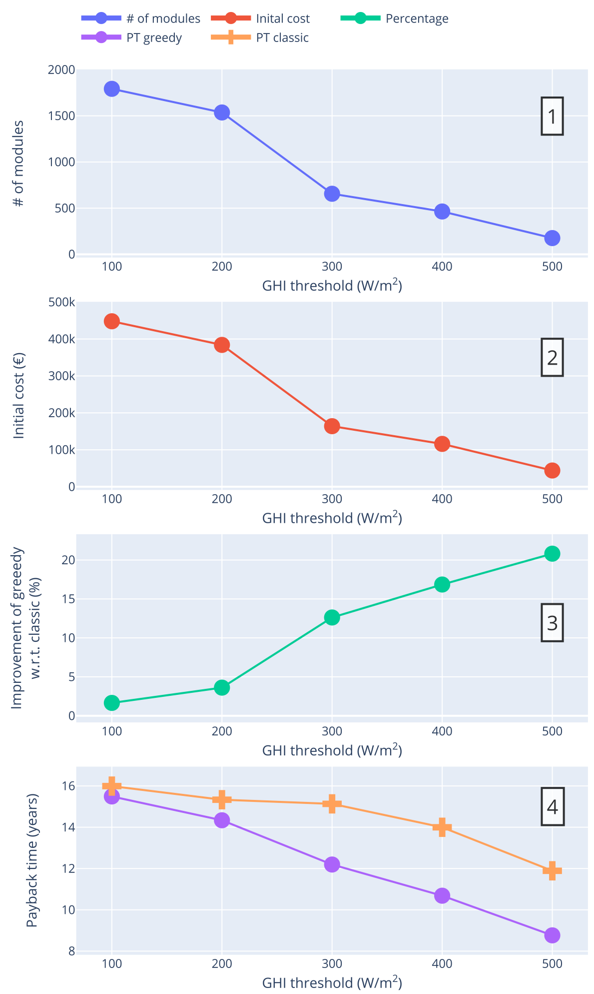

Fig. 5. Behavior of the placement algorithm with different values of $minTh$: number of PV modules (1), initial installation cost (2), improvement of power production w.r.t. the traditional placement (3), payback time (4) (purple for the proposed algorithm, orange for the traditional placement).

roofs ($\sim 0.5\%$ of total district area). The data is then used to build an optimal placement of PV modules, that can be parametrized to exclude positions affected by shading and by a discontinuous irradiance over time. The determined placement allows to find the suitable trade-off between initial investment, power production and payback time of the installation, and proved to generate a surplus power production of up to $+20\%$ w.r.t. a traditional installation.

As future works, we plan to extend the proposed solution by including new constraints, such as i) limiting the maximum number of PV modules to install according to the user's budget and ii) limiting the PT to a maximum value defined by the user.

References

[1] "Future of solar photovoltaic - deployment, investment, technology, grid integration and socio-economic aspects," https://irena.org, IRENA - International Renewable Energy Agency, Tech. Rep., 2019.

[2] S. Milčiuviene, J. Kiršiene, E. Doheijo, R. Urbonas, and D. Milčius, "The role of renewable energy prosumers in implementing energy justice theory," *Sustainability*, vol. 11, no. 19, 2019.

[3] X. Lu, K. Li, H. Xu, F. Wang, Z. Zhou, and Y. Zhang, "Fundamentals and business model for resource aggregator of demand response in electricity markets," *Energy*, vol. 204, p. 117885, 2020.

[4] "New business model encourages escos to join forces with demand response aggregators," https://ec.europa.eu/easme/en/news/new-business-model-encourages-escos-join-forces-demand-response-aggregators, European Commission, Executive Agency for SMEs (EASME), Tech. Rep., Jun 2020.

[5] L. Zhu, Q. Li, M. Chen, K. Cao, and Y. Sun, "A simplified mathematical model for power output predicting of Building Integrated Photovoltaic under partial shading conditions," *Elsevier Energy Conversion and Management*, vol. 180, pp. 831–843, 2019.

[6] M. A. Masoum, S. M. M. Badejani, and M. Kalantar, "Optimal placement of hybrid pv-wind systems using genetic algorithm," in *2010 Innovative Smart Grid Technologies (ISGT)*. IEEE, 2010, pp. 1–5.

[7] A. D. Ondeck, T. F. Edgar, and M. Baldea, "Optimal operation of a residential district-level combined photovoltaic/natural gas power and cooling system," *Applied Energy*, vol. 156, pp. 593–606, 2015.

[8] S. Chowdhury and T. Matlokotsi, "Optimal placement and sizing of renewable distributed generation in electricity networks considering different load models," in *Proc. of International Universities Power Engineering Conference (UPEC)*, 2017, pp. 1–6.

[9] S. Kucuksari, A. M. Khaleghi, M. Hamidi, Y. Zhang, F. Szidarovszky, G. Bayraksan, and Y.-J. Son, "An integrated gis, optimization and simulation framework for optimal pv size and location in campus area environments," *Applied Energy*, vol. 113, pp. 1601–1613, 2014.

[10] B. Pillot, N. Al-Kurdi, C. Gervet, and L. Linguet, "An integrated gis and robust optimization framework for solar pv plant planning scenarios at utility scale," *Applied Energy*, vol. 260, p. 114257, 2020.

[11] A. Yushchenko, A. De Bono, B. Chatenoux, M. K. Patel, and N. Ray, "GIS-based assessment of photovoltaic (PV) and concentrated solar power (CSP) generation potential in West Africa," *Renewable and Sustainable Energy Reviews*, vol. 81, pp. 2088–2103, 2018.

[12] N. H. Baranyai, H. Zsiborács, A. Vincze, N. Rodek, M. Makai, G. Pintér *et al.*, "Correlation analysis of the spread of household-sized photovoltaic power plants and various district indicators: A case study," *Sustainability*, vol. 13, no. 2, pp. 1–1, 2021.

[13] W. Khemiri, R. Yaagoubi, and Y. Miky, "Optimal placement of solar photovoltaic farms using analytical hierarchical process and geographic information system in mekkah, saudi arabia," in *AIP Conference Proceedings*, vol. 2056, no. 1. AIP Publishing LLC, 2018, p. 020025.

[14] L. Bergamasco and P. Asinari, "Scalable methodology for the photovoltaic solar energy potential assessment based on available roof surface area: Application to piedmont region (italy)," *Solar energy*, vol. 85, no. 5, pp. 1041–1055, 2011.

[15] S. Bracco, F. Delfino, G. Ferro, L. Pagnini, M. Robba, and M. Rossi, "Energy planning of sustainable districts: Towards the exploitation of small size intermittent renewables in urban areas," *Applied Energy*, vol. 228, pp. 2288–2297, 2018.

[16] S. Vinco, L. Bottaccioli, E. Patti, A. Acquaviva, E. Macii, and M. Poncino, "GIS-based optimal photovoltaic panel floorplanning for residential installations," in *Proc. of Design, Automation Test in Europe Conference Exhibition (DATE) 2018*, pp. 437–442.

[17] R. El Kontar and X. Jin, "Optimal efficiency and operational cost savings: A framework for automated rooftop pv placement," in *Proceedings of 2020 Building Performance Analysis Conference and SimBuild, ASHRAE and IBPSA-USA*, 2020.

[18] "PV-MF165EB3 (165Wp) PV module," https://www.mitsubishielectricsolar.com/images/uploads/documents/specs/L-175-4-B6504-A_MF165EB3.pdf, Mitsubishi Electric, 2004.

[19] Q. Li, L. Zhu, Y. Sun, L. Lu, and Y. Yang, "Performance prediction of building integrated photovoltaics under no-shading, shading and masking conditions using a multi-physics model," *Elsevier Energy*, vol. 213, p. 118795, 2020.

[20] "GDAL — GDAL documentation." [Online]. Available: https://gdal.org/

[21] R. Margolis, P. Gagnon, J. Melius, C. Phillips, and R. Elmore, "Using GIS-based methods and lidar data to estimate rooftop solar technical potential in US cities," *Environmental Research Letters*, vol. 12, 2017.

[22] L. Bottaccioli, E. Patti, E. Macii, and A. Acquaviva, "GIS-based software infrastructure to model PV generation in fine-grained spatio-temporal domain," *IEEE Systems Journal*, vol. 12, no. 3, pp. 2832–2841, 2018.

[23] "Electricity price statistics - Statistics Explained," https://ec.europa.eu/eurostat/statistics-explained/index.php/Electricity_price_statistics.